Incorporation Kinetics of Lysolecithin into Lecithin Vesicles. Kinetics of Lysolecithin-Induced Vesicle Fusion†

Khalid Elamrani and Alfred Blume*

ABSTRACT: The incorporation kinetics of 1-palmitoylphosphatidylcholine (lysolecithin) into dimyristoyl- and dipalmitoylphosphatidylcholine vesicles and the subsequent aggregation and fusion of the vesicles into larger aggregates were studied by using stopped-flow rapid-mixing techniques. The half-times for the lysolecithin incorporation vary between 50 and 500 ms. The incorporation rate has a maximum in the temperature range of the vesicle phase transition. This process is not diffusion controlled. The rate-limiting step is the incorporation of the lysolecithin monomer into the lipid bilayer. After this fast process, a slow reaction in the 10–50-min time range is observed. The large irreversible increase in turbidity indicates aggregation and fusion of the vesicles. The initial step is a second-order reaction with respect to the vesicle concentration, indicating aggregation or fusion of two vesicles. The aggregation rate passes through a maximum at the phase transition temperature.

Biological membranes generally contain only small amounts of lysophospholipids (van Deenen, 1965). As intermediates in the lipid metabolism they are either quickly degraded or reacylated to the respective diester phospholipids (Mulder et al., 1963; Robertson & Lands, 1964). These reactions are very important for the cell because larger amounts of lysolipids eventually lead to a disruption of the cell (Delezenne & Ledebt, 1911; Manwaring, 1910). While this lytic action of lysolipids was observed a long time ago, a systematic study of the action of lysolipids could not be started until enzyme-resistent lysolipid analogues were available [Arnold & Weltzien, 1968; Reman et al., 1969; for review, see Weltzien (1979)]. On the basis of these investigations, it was suggested that several reaction steps are involved in cell lysis: (a) adsorption of the lysolipid to the cell surface, (b) incorporation into the cell membrane, (c) diffusion in the plane of the membrane with subsequent perturbation of the lipid–protein and/or protein–protein interactions, which then lead to changes in membrane permeability, and (d) permeation of water into the cell with subsequent disruption of the cell membrane. Whereas large amounts of lysolipids generally have lytic effects, smaller amounts can lead to cell fusion [Poole et al., 1970; Croce et al., 1971; for review, see Gratzl et al. (1980)] or to a faster immune response (Munder et al., 1973). The aim of our study was to shed light onto the mechanism of lysolecithin incorporation into lipid bilayers. As a model system, we choose DMPC[1] and DPPC single-walled vesicles and measured the incorporation rate of LPC into these vesicles by using the stopped-flow technique. Of special interest was the effect of temperature and the influence of the phase transition on the incorporation kinetics.

Experimental Procedures

Materials. DMPC, DPPC, and LPC[1] were purchased from FLUKA (Neu-Ulm, West Germany) and used without further purification. Their purity as checked by TLC was ~98%.

Methods. Phospholipid vesicles were prepared according to Kremer et al. (1977). An ethanolic phospholipid solution (0.8 mL) (c = 20–30 mM) was injected into 14 mL of buffer solution (0.1 M NaCl and 0.01 M Tris-HCl, pH 7.3) at a temperature above the respective phase transition temperature of the lipid. The injection rate was 0.04 mL/min. Aliquots of the stock vesicle suspension were diluted to the appropriate concentration needed for the experiment and dialyzed against pure buffer for at least 12 h to remove residual ethanol. However, our experiments showed that small amounts of ethanol had no measurable effect on the reaction rates.

The size of the vesicles was determined by light-scattering measurements using a Sofica light-scattering spectrometer. Intensities of scattered light at 436 nm were measured between 20° and 135° using 5° steps. The temperature was kept constant to 30 °C for DMPC and 50 °C for DPPC vesicles. Turbidity vs. temperature curves were measured with a PYE UNICAM SP 1800 spectrophotometer with variable temperature cell holder heated with a PYE UNICAM SP 876 temperature controller. The turbidity was recorded at 360 nm, and the scan rate used was 1 °C/min. Kinetic measurements were made by using a Durrum 110 stopped-flow apparatus with optical detection (360 nm). The temperature of the reactants was kept constant to ±0.5 °C by using a MGW Lauda thermostat. The time dependence of the absorbance was recorded with a Datalab DL 905 transient recorder and displayed on a Tektronix 7704 oscilloscope. Turbidity vs. time curves were stored in a home-built 64K solid-state memory (G. Messner, Institut fur physikalische Chemie, Freiburg) and subsequently read into a Hewlett-Packard 9845 computer for the evaluation of the time constants. In some cases when only small turbidity changes were encountered, ~16 curves were averaged to increase the signal to noise ratio.

Results

The phospholipid vesicles used for the stopped-flow measurements were characterized by light-scattering measurements. In accordance with the observations by Kremer et al. (1977), the vesicle size depends on the lipid concentration in the ethanolic solution. Lipid concentrations between 20 and 30 mM gave vesicles with a radius between 35 and 50 nm. Vesicles of this size proved to be stable to the shear forces during the rapid-mixing process. In experiments where the

† From the Institut für Physikalische Chemie II, D-7800 Freiburg, Federal Republic of Germany. *Received May 19, 1981.* This work was supported by the Deutsche Forschungsgemeinschaft.

[1] Abbreviations: DMPC, dimyristoylphosphatidylcholine; DPPC, dipalmitoylphosphatidylcholine; LPC, 1-palmitoylphosphatidylcholine; TLC, thin-layer chromatography; Tris, tris(hydroxymethyl)aminomethane.

0006-2960/82/0421-0521$01.25/0

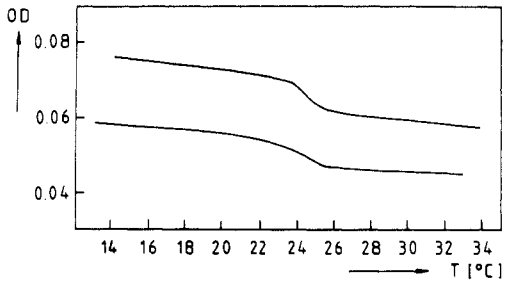

FIGURE 1: Temperature dependence of the optical density (λ = 360 nm) of a suspension of pure DMPC vesicles (c_{DMPC} = 0.81 mM, lower curve) and of DMPC/LPC vesicles (c_{DMPC} = 0.81 mM and c_{LPC} = 0.16 mM, upper curve) in buffer, pH 7.25 (0.01 M Tris and 0.1 M NaCl).

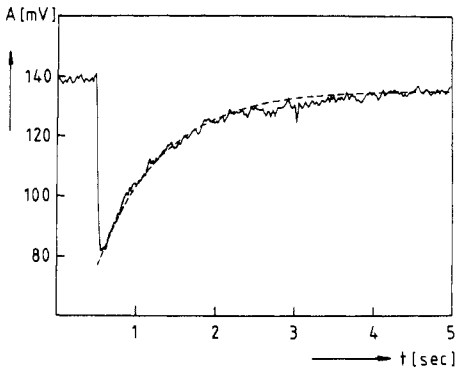

FIGURE 2: Time course of the absorbance (photomultiplier voltage 10 mV = 0.001 A) after mixing of equal volumes of a DMPC vesicle solution (c_{DMPC} = 1.14 mM) and a LPC solution (c_{LPC} = 0.23 mM) at a temperature of 15 °C. The dotted line is a computer fit using a single exponential.

vesicle suspensions were mixed with buffer, no turbidity changes were observed. Turbidity vs. temperature curves of DMPC vesicles with and without 16.6 mol % LPC are shown in Figure 1. As is well known, the transition temperature for vesicles is slightly lower, and the transition is broader. The transition is only slightly affected by the addition of LPC. Similar observations have been reported for multilamellar dispersions (Klopfenstein et al., 1974).

The kinetics of the LPC incorporation into DMPC and DPPC vesicles were studied in a broad temperature range including the phase transition region. Unfortunately, precise stopped-flow measurements above the DPPC transition temperature were not possible due to low signal to noise ratios and the formation of gas bubbles during the mixing process, despite the degassing of the vesicle suspensions prior to the experiments. Figure 2 shows a representative turbidity vs. time curve of a stopped-flow experiment. Equal volumes of 1.14 mM DMPC vesicle suspension and a 0.23 mM LPC solution were mixed (T = 15 °C). The mixing is followed by a rapid drop in turbidity. The subsequent incorporation of the LPC molecules leads to an exponential increase in the turbidity, because the molecular weight and the size of the vesicles increase. (The turbidity arising from the LPC micelles can be neglected because of their small size and molecular weight.) The turbidity increase follows a single exponential, and a semilogarithmic plot gives essentially a straight line. (The subsequent slow reaction with large turbidity increase—not shown in Figure 2—will be described below.) The relative increase in turbidity depends on the amount of added LPC. It shows only a slight temperature dependence; 16.6 mol % LPC increases the turbidity by 9–14% between 5 and 50 °C.

The experimental rate constants $k_{exptl} = \ln 2/t_{1/2}$ for the incorporation of LPC into DMPC vesicles at four different

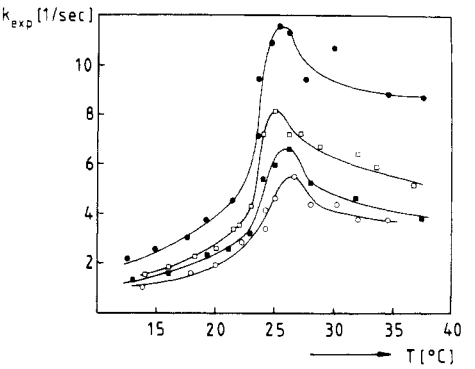

FIGURE 3: Rate constant k_{exptl} as a function of temperature for DMPC vesicles containing 16.6 mol % LPC. (●) c_{DMPC} = 0.81 mM; (□) c_{DMPC} = 0.54 mM; (■) c_{DMPC} = 0.41 mM; (○) c_{DMPC} = 0.27 mM.

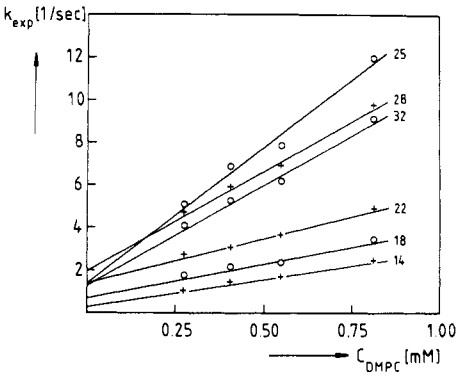

FIGURE 4: Plot of k_{exptl} vs. c_{DMPC} for DMPC vesicles containing 16.6 mol % LPC. Numbers indicate temperatures in °C.

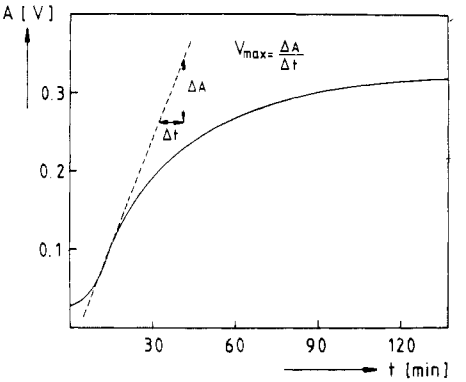

FIGURE 5: Optical absorbance at 360 nm vs. time (1 V = 0.9 A) for a DPPC/LPC vesicle suspension (c_{DPPC} = 0.54 mM, c_{LPC} = 0.108 mM, and T = 39 °C).

DMPC vesicle concentrations are plotted in Figure 3. The incorporation rate depends strongly on temperature and has a pronounced maximum at the high temperature end of the vesicle phase transition. When the k_{exptl} values are plotted vs. the DMPC vesicle concentration (Figure 4) a linear relation is obtained. This indicates that the observed process is pseudo first order. The LPC incorporation into DPPC vesicles is essentially similar and was not investigated systematically. On a reduced temperature scale, the incorporation of LPC into DPPC vesicles is faster by a factor of 5, and on the absolute temperature scale, however, the reaction is slower by a factor of 2 when both lipids are compared below their respective phase transition temperatures.

The subsequent irreversible reaction is slow with half-times between 10 and 50 min and is accompanied by a large turbidity increase, indicating aggregation and fusion of the vesicles to larger particles. This aggregation can be studied in a conventional spectrophotometer after premixing the reactants in

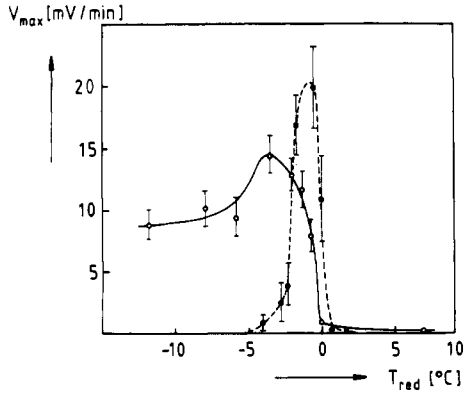

FIGURE 6: Reaction rate V_{max} as function of $T_{red} = T - T_m$ for vesicles containing 16.6 mol % LPC. (○) DMPC; (●) DPPC. Vertical bars represent standard deviations.

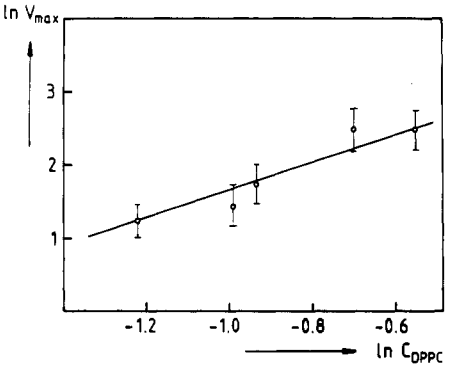

FIGURE 7: Double logarithmic plot of V_{max} vs. c_{DPPC} for DPPC vesicles containing 16.6 mol % LPC at T = 39 °C.

the sample cell (see Figure 5). The reaction is complex. A short lag phase is followed by a large increase in the turbidity which gradually levels off. The end point of the aggregation could not be observed because the dispersions tended to settle when the particles had grown large enough. Only the initial faster increase in the turbidity was considered in our kinetic analysis, because in the region of low turbidity the particles are small enough so that interference effects can be neglected. Figure 6 shows a plot of V_{max} obtained from turbidity curves vs. the temperature. DMPC and DPPC vesicles show distinctively different behavior. Whereas for both lipids maximal rates are observed at the transition midpoint, only DMPC vesicles show appreciable fusion outside the phase transition region. The reaction order can be found from the dependence of V_{max} on the vesicle concentration. Figure 7 shows a double logarithmic plot V_{max} vs. c_{DPPC}. A linear relation with a slope of ~2 is obtained. The initial phase of the vesicle aggregation is thus second order with respect to the vesicle concentration. When the LPC concentration is changed relative to the DPPC concentration, V_{max} increases linearly up to 20% LPC (see Figure 8). The deviation from linearity at higher LPC concentration seems to indicate a change in the reaction mechanism.

Discussion

(A) Kinetics of LPC Incorporation. The observed turbidity increase after mixing can be explained by the incorporation of LPC molecules into the vesicles, thus increasing their size and weight but leaving the number of vesicles constant. A quantitative relation between vesicle size and specific turbidity has been calculated by Chong & Colbow (1976). Using the results of these calculations, we would expect roughly a 14% increase of the turbidity when all LPC molecules were incorporated. This would increase the vesicle radius for instance

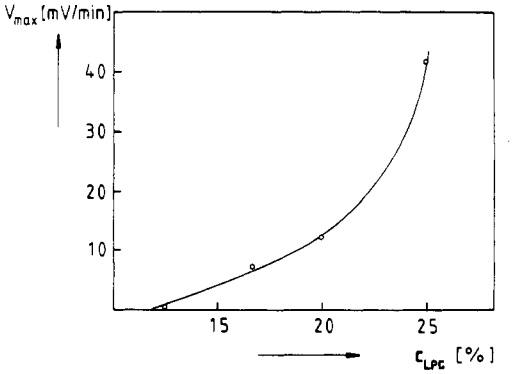

FIGURE 8: V_{max} vs. c_{LPC} (in % of c_{DPPC}). c_{DPPC} = 0.81 mM at T = 39 °C.

from 44 to 48 nm and the molecular weight of the vesicle by 11% (final LPC concentration 16.6%). We indeed find approximately the predicted values (9–14%), with the lower ones being observed below the phase transition of the vesicles. Obviously LPC partitions more easily into the bilayers above the transition. Because the radius of the vesicles increases only slightly, the turbidity is directly proportional to the weight of the vesicle and thus to the number of LPC molecules incorporated. As already mentioned before, the turbidity resulting from the LPC micelles can be neglected because of their small molecular weight as compared to the vesicle weight, characteristically ~10%. The turbidity change after mixing follows a single exponential (see Figure 2). Moreover the experimental rate constants show a linear dependence on the vesicle concentration. Thus the following equation can be formulated for the overall reaction:

$$\underset{a}{V} + \underset{b}{LPC(f)} \underset{k_{ba}}{\overset{k_{ab}}{\rightleftharpoons}} \underset{c}{V{\cdot}LPC(inc)} \qquad (1)$$

where a = V = PC – vesicle, b = LPC(f) = free LPC molecules, and c = LPC(inc) = incorporated LPC molecules. Using the above abbreviations, we have at equilibrium

$$k_{ba}c_\infty = k_{ab}a_\infty b_\infty \qquad (2)$$

where a_∞, b_∞, and c_∞ = equilibrium concentrations of components a, b, and c. Because the concentration of component a (the vesicles) does not change, $a = a_0 = a_\infty$, so that we obtain for the initial concentration b_0:

$$b_0 = c_\infty + b_\infty = c_\infty + \frac{k_{ba}c_\infty}{k_{ab}a_0} \qquad (3)$$

From eq 1 and 3 we get for the rate of incorporation

$$\begin{aligned} dc/dt &= k_{ab}ab - k_{ba}c \\ &= k_{ab}a_0(b_0 - c) - k_{ba}c \\ &= (k_{ab}a_0 + k_{ba})(c_\infty - c) \end{aligned} \qquad (4)$$

Integration then gives

$$\ln \frac{c_\infty - c}{c_\infty - c_0} = (k_{ab}a_0 + k_{ba})t \qquad (5)$$

A plot of ln $(c_\infty - c)$ vs. t should give a straight line with a slope of $k_{exptl} = k_{ab}a_0 + k_{ba}$. This was indeed observed. From

$$k_{exptl} = k_{ab}a_0 + k_{ba} = k_{ab}[V] + k_{ba} = (k_{ab}/N_{PC})[PC] + k_{ba} \qquad (6)$$

where N_{PC}, the number of phosphatidylcholine molecules per vesicle can be calculated from the known vesicle radius, we determined the rate constants k_{ab} and k_{ba} by using the data of Figure 4. The results are shown in Table I (and Figure 9).

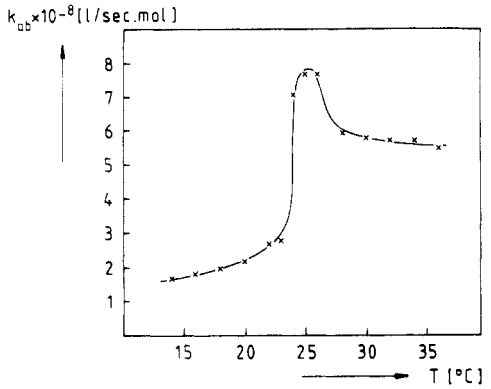

FIGURE 9: Temperature dependence of rate constant k_{ab} (data from Table I).

Table I: Rate Constants k_{ab} and k_{ba} Calculated with Data from Figure 4 and Equation 6[a]

temp (°C)	k_{ab}/N_{PC} ($\times 10^{-3}$) (L mol^{-1} s^{-1})	k_{ab} ($\times 10^{-8}$) (L mol^{-1} s^{-1})	k_{ba} ($\times 10^{-3}$) (s^{-1})
14	2.60	1.61	0.21
18	3.10	1.92	0.72
22	4.26	2.64	1.38
25	12.34	7.65	1.39
28	9.50	5.89	1.90
32	9.16	5.68	1.28

[a] $N_{PC} = 6.2 \times 10^4$.

We want to interpret these results assuming the following reaction steps: (1) diffusion of the LPC monomer to the PC vesicle and subsequent adsorption and (2) incorporation of the LPC monomer into the vesicle bilayer. Because the monomer exchange equilibrium between the LPC micelles and the monomers in solution is reached much faster than the consecutive reactions occur (Thomas et al., 1977), this reaction can be neglected in the kinetic equations. The last step in the reaction sequence, the equilibration of the LPC molecules in the vesicle by lateral and transverse diffusion, cannot be observed in our experiments because no weight change of the vesicle occurs in this process so that the turbidity does not change. Considering only the intermediate steps, eq 1 could be extended to

$$V + LPC(f) \underset{k_{21}}{\overset{k_{12}}{\rightleftharpoons}} [V{\cdot}LPC(b)] \underset{k_{32}}{\overset{k_{23}}{\rightleftharpoons}} V{\cdot}LPC(inc) \quad (7)$$

where LPC(b) = bound LPC monomer. The first diffusion-controlled step can be calculated by using the Smoluchowski equation (Smoluchowski, 1917). For uncharged particles, the rate constants for a bimolecular collision can be expressed in terms of the collision radius r_{AB} and the diffusion coefficients D_A and D_B of the reacting species:

$$k_{12} = k_{coll} = (4\pi N_A/1000)(D_A + D_B)r_{AB} \quad (8a)$$

$$k_{21} = k_{sep} = 3(D_A + D_B)/r_{AB}^2 \quad (9a)$$

where N_A is Avogadros number. These equations can be simplified in our case. Because the vesicles are very large compared to the LPC monomers, their diffusion is negligible. Likewise the collision radius r_{AB} can be replaced by the vesicle radius r_V:

$$k_{12} = (4\pi N_A/1000)D_{LPC}r_V \quad (8b)$$

$$k_{21} = 3D_{LPC}/r_V^2 \quad (9b)$$

Inserting the appropriate values for r_V and D_{LPC} (r_V = 44 nm and $D_{LPC} \simeq 5 \times 10^{-6}$ cm^2/s), we find $k_{12} = 1.7 \times 10^{11}$ L mol^{-1} s^{-1} and $k_{21} = 3.4 \times 10^6$ s^{-1}. A comparison with the k_{ab} and k_{ba} values in Table I shows that these are by $\sim$3 orders of magnitude lower. We conclude that the diffusion of the LPC monomer cannot be the rate-determining step. It is therefore justified to apply a steady-state approximation for the intermediate product in eq 7. This leads to the following expression for k_{exptl}:

$$k_{exptl} = [k_{23}k_{12}/(k_{21} + k_{23})][V] + k_{32}k_{21}/(k_{23} + k_{21}) \quad (10)$$

With $k_{23} \ll k_{12}$ and k_{21} and by comparison with eq 6

$$k_{ab} = k_{23}k_{12}/k_{21} \quad (11)$$

Table II: Rate Constant k_{23} and Fraction $x = k_{23}/(k_{23} + k_{21})$

temp (°C)	k_{ab}[a] ($\times 10^{-8}$) (L mol^{-1} s^{-1})	k_{23}[b] ($\times 10^{-3}$) (s^{-1})	$k_{23}/(k_{23} + k_{21})$ ($\times 10^3$)
14	1.61	2.95	0.87
25	7.65	15.30	4.50
32	5.68	11.36	3.34

[a] Data from Table I. [b] Calculated according to eq 11 with $k_{12} = 1.7 \times 10^{11}$ L mol^{-1} s^{-1} and $k_{21} = 3.4 \times 10^6$ s^{-1}.

Table II shows the calculated k_{23} values by using eq 11, the k_{ab} values from Table I, and the approximated rate constants k_{12} and k_{21} (see above). Table II also includes the fraction of the collision complexes $x = k_{23}/(k_{23} + k_{21})$ which leads to the incorporation of LPC. Only 1 out of 1000 collisions leads to an incorporation of an LPC monomer. Another piece of strong evidence speaking against a diffusion-controlled reaction is the observed temperature dependence of the rate constants. A diffusion-controlled mechanism should lead to a continuous change of the rate constant with temperature because the reaction rate is determined by the viscosity of the solvent. However, we observe a pronounced maximum of the rate constants in the temperature region of the vesicle phase transition. Similar kinetic behavior was found before for the permeation of ions and small molecules through lipid bilayers (Papahadjopoulos et al., 1973; Wu & McConnell, 1973; Tsong, 1975; Phillips et al., 1975; Marsh et al., 1976; Blok et al., 1975). In accordance with these previous findings we suggest that the LPC incorporation rate is determined by density fluctuations in the lipid bilayer.

In the phase transition region, bilayers as well as monolayers have high lateral compressibility, and the density fluctuations go through a maximum (Phillips et al., 1975; Linden et al., 1973; Nagle & Scott, 1978; Mitaku et al., 1978). Following the fast adsorption step, the LPC incorporation is thus facilitated when the bilayer is in a state of high lateral compressibility. Because the compressibility in the gel state is lower than in the liquid-crystalline state, this would also explain the larger rate constants found above the vesicle phase transition. An alternative explanation for the maximum in the rate constants would be to assume that LPC molecules are preferentially incorporated into bilayer defects. The phase boundaries between gel and liquid-crystal phase domains in the phase transition region lead to a larger number of defects and thus to a facilitated incorporation. This mechanism has been proposed by Marsh et al. (1976) for the transport of tempocholine across DMPC bilayers. Kanehisa & Tsong (1978) suggested a cluster model for the phase transition of lipids and applied it to calculate permeation of hydrophilic and hydrophobic molecules through the bilayer. The LPC incorporation would fall into the type 2 behavior of their model; i.e., the LPC molecules are preferentially incorporated into cluster boundaries.

It should be mentioned that only polar and amphiphilic molecules seem to show this particular kind of kinetic behavior with a maximum at the phase transition temperature. Nonpolar molecules show a more or less continuous increase in the incorporation rate with temperature (Tsong, 1975; Woolley & Diebler, 1979). Woolley & Diebler (1979) could show that the incorporation of the nonpolar fluorescent probe *N*-phenylnaphthylamine is in fact a diffusion-controlled process.

(*B*) *Kinetics of Vesicle Growth.* The fusion of membranes is an important process in biological systems (Poste & Allison, 1973; Gratzl et al., 1980). Considerable effort has been made to study the mechanism of membrane fusion applying phospholipid vesicles as model systems (Papahadjopoulos et al., 1976; Kantor & Prestegard, 1975, 1978; Martin & McDonald, 1976; Kremer & Wiersema, 1977; Liao & Prestegard, 1980). The vesicle growth observed in these model systems has either been interpreted as direct fusion of monobilayer vesicles or as an exchange process of lipid monomers through the water phase, where the monomers are preferentially incorporated into the larger vesicles. The growth process we observe after the addition of LPC depends on the vesicle concentration and turns out to be a second-order reaction in the initial phase (see Figure 7). It seems to be appropriate and in accordance with observations in other systems (Martin & McDonald, 1976) to assume at least for the initial phase of the growth reaction a simple aggregation of two vesicles with subsequent irreversible fusion:

$$V + V \underset{k_{21}}{\overset{k_{12}}{\rightleftharpoons}} [VV] \xrightarrow{k_{23}} V_2 \qquad (12)$$

This reaction mechanism with a consecutive reaction leading to V_2 would give a time dependence for the concentration of V_2 qualitatively in agreement with the experimentally observed turbidity changes (see Figure 5). Moreover this mechanism gives a second-order reaction in V. The rate constants k_{12} and k_{21} for the first step can be approximated by using the Smoluchowski equation because the radius of the vesicles is known and the diffusion coefficient of the vesicles can be calculated from the Stokes–Einstein equation. The half-time for the diffusion-controlled collision reaction turns out to be 4 orders of magnitude smaller than that the experimentally observed. Because the rate V_{max} depends on the state of the lipid in the bilayer, i.e., whether it is in the gel or the liquid-crystalline state (see Figure 6), we suggest a fusion mechanism where the extent of defects and density fluctuations in the bilayer affect the fusion rate. Since we used LPC in our studies, we would expect to induce more defects in DMPC than in DPPC bilayers because of the chain length difference between DMPC and LPC. Indeed it was found by differential scanning calorimetry that LPC mixes ideally with DPPC (van Echteld et al., 1980) while it shows nonideal mixing behavior with DMPC (A. Blume, unpublished observations). DPPC vesicles show very little fusion outside the transition range, whereas DMPC vesicles indeed show appreciable fusion at all temperatures (see Figure 6). The considerably faster fusion rate of the DMPC vesicles in the gel state can be explained following similar arguments. It is known that the nonidealities in the mixing behavior are generally larger in the gel than in the liquid-crystalline phase (von Dreele, 1978). In the case of DMPC vesicles, two effects influencing the fusion rate overlap: in the gel phase the incorporation of LPC leads to an increased number of defects, making them more susceptible to fusion, and in the phase transition region formation of phase boundaries between gel and liquid-crystalline domains increases the fusion rate. This overlap leads to the observed asymmetry in the V_{max} vs. temperature curve and to the shift of the maximum fusion rate to the lower end of the phase transition region. For fusion to occur it seems likely that two vesicles have to collide in such a way that at least one defect is located in the area where the two vesicles make contact. This kind of mechanism would explain the observed linear increase of the fusion rate with the LPC concentration in the vesicle, because the number of defects should be directly proportional to the number of LPC monomers incorporated.

It should be noted that we cannot determine the exact nature of the initial aggregation reaction. In particular, we do not know whether the following irreversible fusion of the vesicles to larger aggregates proceeds without rupturing the vesicles and causing leakage of vesicle contents. However, the increased number of defects in the bilayer due to the lysolecithin incorporation will increase the permeability, so that membranes become more leaky. Thus a complete preservation of the vesicle contents during lysolecithin-induced aggregation and fusion seems unlikely. The mechanism for the lysolecithin-induced fusion of liposomes with intact cell membranes (Breisblatt & Ohki, 1975; Papahadjopoulos et al., 1976), however, may well be the same as for vesicle–vesicle fusion; i.e., lysolecithin-induced defects act as nucleation sites for fusion. The use of lysolecithin for inducing cell fusion, on the other hand, seems to be of limited value because fusion and lysis are generally found in a very close concentration range (Weltzien, 1979).

Acknowledgments

We thank Professor Dr. Th. Ackermann for his stimulating support and advice.

References

Arnold, D., & Weltzien, H. U. (1968) *Z. Naturforsch. B: Anorg. Chem., Org. Chem., Biochem., Biophys., Biol. 23B*, 675.

Blok, M. C., van der Neut-Kok, E. C. M., van Deenen, L. L. M., & de Gier, J. (1975) *Biochim. Biophys. Acta 406*, 187.

Breisblatt, W., & Ohki, S. (1975) *J. Membr. Biol. 23*, 385.

Chong, C. S., & Colbow, K. (1976) *Biochim. Biophys. Acta 436*, 260.

Croce, C. M., Sawicki, W., Kritchevsky, D., & Koprowski, H. (1971) *Exp. Cell Res. 67*, 427.

Delezenne, C., & Ledebt, J. (1911) *C.R. Hebd. Seances Acad. Sci. 153*, 81.

Gratzl, M., Schudt, C., Ekerdt, R., & Dahl, G. (1980) in *Membrane Structure and Function* (Bittar, E. E., Ed.) Vol. 3, p 59, Wiley, New York.

Kanehisa, I. M., & Tsong, T. Y. (1978) *J. Am. Chem. Soc. 100*, 424.

Kantor, H. L., & Prestegard, J. H. (1975) *Biochemistry 14*, 1790.

Kantor, H. L., & Prestegard, J. H. (1978) *Biochemistry 17*, 3592.

Klopfenstein, W. E., de Kruijff, B., Verkleij, A. J., Demel, R. A., & van Deenen, L. L. M. (1974) *Chem. Phys. Lipids 13*, 215.

Kremer, J. M. H., & Wiersema, P. H. (1977) *Biochim. Biophys. Acta 471*, 348.

Kremer, J. M. H., van der Esker, M. W. J., Pathamamanahoran, C., & Wiersema, P. H. (1977) *Biochemistry 16*, 3932.

Liao, Y., & Prestegard, J. H. (1980) *Biochim. Biophys. Acta 599*, 81.

Linden, C. D., Wright, K. L., McConnell, H. M., & Fox, C. F. (1973) *Proc. Natl. Acad. Sci. U.S.A. 70*, 2271.

Manwaring, W. H. (1910) *Z. Immunitaetsforsch. 6*, 513.
Marsh, D., Watts, A., & Knowles, P. F. (1976) *Biochemistry 15*, 3570.
Martin, F. J., & McDonald, R. C. (1976) *Biochemistry 15*, 321.
Mitaku, S., Ikegami, A., & Sakanishi, A. (1978) *Biophys. Chem. 8*, 295.
Mulder, E., de Gier, I., & van Deenen, L. L. M. (1963) *Biochim. Biophys. Acta 20*, 94.
Munder, P. G., Modolell, M., Raetz, W., & Luckenbach, G. A. (1973) *Eur. J. Immunol. 3*, 454.
Nagle, J. F., & Scott, H. L. (1978) *Biochim. Biophys. Acta 513*, 236.
Papahadjopoulos, D., Jacobson, K., Nir, S., & Isac, T. (1973) *Biochim. Biophys. Acta 311*, 330.
Papahadjopoulos, D., Nui, S., Vail, W. I., & Poste, G. (1976) *Biochim. Biophys. Acta 448*, 245.
Phillips, M. C., Graham, D. E., & Hauser, H. (1975) *Nature (London) 254*, 154.
Poole, A. R., Howell, J. I., & Lucy, J. A. (1970) *Nature (London) 227*, 810.
Poste, G., & Allison, A. C. (1973) *Biochim. Biophys. Acta 300*, 421.
Reman, R. C., Demel, R. A., de Gier, J., van Deenen, L. L. M., Eibl, H., & Westphal, D. (1969) *Chem. Phys. Lipids 3*, 221.
Robertson, A. F., & Lands, W. E. M. (1964) *J. Lipid Res. 5*, 88.
Smoluchowski, M. (1917) *Z. Phys. Chem., Stoechiom. Verwandtschaftsl. 92*, 129.
Thomas, J. K., Grieser, F., & Wong, M. (1977) *Ber. Bunsenges. Phys. Chem. 82*, 937.
Tsong, T. Y. (1975) *Biochemistry 14*, 5409.
van Deenen, L. L. M. (1965) *Prog. Chem. Fats Other Lipids 8* (*Part* 1), 17-33.
van Echteld, C. J. A., de Kruijff, B., & de Gier, J. (1980) *Biochim. Biophys. Acta 595*, 71.
von Dreele, P. H. (1978) *Biochemistry 17*, 3939.
Weltzien, H. U. (1979) *Biochim. Biophys. Acta 559*, 259.
Woolley, P., & Diebler, H. (1979) *Biophys. Chem. 10*, 305.
Wu, S., & McConnell, H. M. (1973) *Biochem. Biophys. Res. Commun. 55*, 484.

Structure and Dynamics of Phospholipid Membranes: An Electron Spin Resonance Study Employing Biradical Probes†

Peter Meier, Alfred Blume, Ernst Ohmes, Franz A. Neugebauer,‡ and Gerd Kothe*

ABSTRACT: The large zero-field splitting of rigid biradicals makes them important candidates for spin probes of phospholipid membranes. Here we develop an electron spin resonance line-shape model for such probes on the basis of the stochastic Liouville equation. Particular emphasis is given to the slow-diffusional regime, characteristic of bilayers in the gel phase. The theory is employed to study the line shapes of bis(verdazyl) biradicals, incorporated into oriented multibilayers of dimyristoylphosphatidylcholine. Computer simulations of the *angular-dependent spectra* provide the orientational distribution functions and rotational correlation times of the spin probes. They occupy two different sites in bilayer membrane. The orientational distribution of the spin probes is related to the structure of the phospholipid phases. In the $L_{\beta'}$ phase the hydrocarbon chains are uniformly tilted by $\delta = 23°$ with respect to the bilayer normal. For the $P_{\beta'}$ phase we observe a random distribution of tilt angles from $\delta = 0°$ to $\delta = 19°$, indicating that the chains orient perpendicular to the local (rippled) bilayer surface. This structure has not been established previously. In agreement with other studies we find no tilt for the L_α phase. The order parameters of the hydrocarbon chains increase with decreasing temperature, jumping from $S \leq 0.6$ to $S \geq 0.8$ at the main transition. From the rotational correlation times of the spin probes, intrinsic bilayer viscosities of $0.08\ P \leq \eta \leq 20\ P$ ($50\ °C \geq T \geq 1\ °C$) are determined. An Arrhenius plot provides activation energies of the viscous flow. The values increase from $E_{visc} \sim 10$ kcal/mol in the L_α phase to $E_{visc} \sim 18$ kcal/mol in the $L_{\beta'}$ phase.

The present knowledge about the physical properties of biological membranes originates to a great extent from studies of model membranes, prepared from natural and synthetic phospholipids. Fully hydrated phosphatidylcholines form bilayer structures, which exist in two distinctly different phases. The nature of the liquid-crystalline phase has been well characterized by different techniques [for a recent review, see Grell (1981)]. The detailed organization of the bilayer in the gel phase is less clearly understood. Particularly, the nature of an endothermic event, generally referred to as the pretransition, is still the subject of discussion.

In the present study we investigate this problem with electron spin resonance spectroscopy (ESR),[1] using rigid biradicals as spin probes. They possess one clear advantage over their monoradical counterparts; for in addition to the Zeeman and hyperfine interaction, there is also the totally anisotropic

† From the Institute of Physical Chemistry, University of Freiburg, D-7800 Freiburg, Federal Republic of Germany. *Received April 2, 1981.* This work was supported by Deutsche Forschungsgemeinschaft and Fonds der Chemischen Industrie.

‡ Present address: Max-Planck-Institut für Medizinische Forschung, Abteilung Organische Chemie, D-6900 Heidelberg, Federal Republic of Germany.

[1] Abbreviations: ESR, electron spin resonance; BVL, 3,3′-(1,4-phenylene)bis(verdazyl); DMPC, dimyristoylphosphatidylcholine; NMR, nuclear magnetic resonance; DPH, 1,6-diphenyl-1,3,5-hexatriene; STESR, saturation transfer electron spin resonance.

0006-2960/82/0421-0526$01.25/0